

From independent particle towards collective motion in two electron square lattices

Moisés Martínez and Jean-Louis Pichard

CEA/DSM, Service de Physique de l'État Condensé, Centre d'Études de Saclay, 91191, Gif sur Yvette cedex, France

february 2002

Abstract. The two dimensional crossover from independent particle towards collective motion is studied using 2 spinless fermions interacting via a U/r Coulomb repulsion in a $L \times L$ square lattice with periodic boundary conditions and nearest neighbor hopping t . Three regimes characterize the ground state when U/t increases. Firstly, when the fluctuation Δr of the spacing r between the two particles is larger than the lattice spacing a , there is a scaling length $L_0 = \sqrt{8\pi^2(t/U)}$ such that the relative fluctuation $\Delta r/\langle r \rangle$ is a universal function of the dimensionless ratio L/L_0 , up to finite size corrections of order L^{-2} . $L < L_0$ and $L > L_0$ are respectively the limits of the free particle Fermi motion and of the correlated motion of a Wigner molecule. Secondly, when U/t exceeds a threshold $U^*(L)/t$, Δr becomes smaller than a , giving rise to a correlated lattice regime where the previous scaling breaks down and analytical expansions in powers of t/U become valid. A weak random potential reduces the scaling length and favors the correlated motion.

PACS. 71.10-w Theories and models for many-electron systems – 71.27+a Strongly correlated electron systems – 73.20.Qt Electron solids

1 Introduction

An important issue in quantum many body theory is to know how one goes from independent particle motion towards collective motion when one decreases the density n_s of electrons repelling each other via a U/r Coulomb repulsion. One can trap the electrons by a positive background of charges (jellium model) unless one uses periodic boundary conditions (2d torus geometry). Many studies [1,2,3,4,5,6,7] assume a parabolic trap, its rotational invariance allowing to decouple the motion of the center of mass from the relative motions. A parabolic confinement has the merit to be realizable using semiconductor heterostructures [6,8] for electrons or electromagnetic fields for cold ions. It has however the disadvantage to yield a non uniform charge density, so that the formation of the electron solid when the confinement becomes weak results from a complicated interplay between edge and bulk orderings [7,9]. This leads us to study a system without edge, having the geometry of a two dimensional torus, where the density is uniform. For a continuous torus, the size of the corresponding Hilbert space is infinite, making the use of a truncated basis unavoidable for a numerical study. A way to avoid such a truncation is to take a lattice model (tight binding approximation). Considering the the simplest limit: the ground state (GS) of two spinless fermions in a square $L \times L$ lattice with periodic boundary conditions (BCs), we give an answer to four questions. Is there a simple one parameter scaling theory of the Fermi-Wigner

crossover? How important are the finite size corrections to this scaling theory? Does the lattice play an important role? How those answers are modified when a weak random potential is included?

The answers can be summarized as follows. In the strong coupling limit, the Coulomb repulsion pushes the spacing $|\mathbf{r}|$ between the two particle to take its maximum value $L/\sqrt{2}$ and its fluctuations Δr become of the order of the lattice spacing a . This gives rise to a strongly correlated lattice regime where analytical expansions in powers of t/U are sufficient to describe the system. For weaker couplings, the relative motion becomes more and more delocalized and the lattice effects become irrelevant. This gives rise to a universal regime characterized by a scaling length $L_0 = \sqrt{8\pi^2(t/U)}$. This length corresponds to the system size for which the extra energy to add a second particle in the system is the same in the Wigner limit ($t = 0$) than in the Fermi limit ($U = 0$). $L < L_0$ is the Fermi limit, $L > L_0$ is the Wigner limit and the Fermi-Wigner crossover takes place when $L = L_0$. In this universal regime, the relative fluctuations $\Delta r/\langle r \rangle = F(L/L_0)$ up to finite size corrections of order L^{-2} . When the site potentials have weak random fluctuations of order W , there is still a regime where one parameter scaling remains valid, $\Delta r/\langle r \rangle$ being characterized by a function $F_W(L/L_W)$ which depends on W . Both $\Delta r/\langle r \rangle$ and the scaling length L_W become smaller, in agreement with the general idea that a weak disorder favors the correlated motion.

2 Lattice model

We consider two electrons with symmetric spin wave functions and antisymmetric orbital wave functions (spinless fermions), free to move in a $L \times L$ lattice with periodic BCs, and interacting via a $U/|\mathbf{r}|$ repulsion. The Hamiltonian reads

$$H = -t \sum_{\langle i,j \rangle} (c_i^\dagger c_j + h.c.) + \sum_i v_i n_i + \frac{U}{2} \sum_{i \neq j} \frac{n_i n_j}{|\mathbf{r}_{ij}|} \quad (1)$$

where i, j label the lattice sites, $\langle i,j \rangle$ means i nearest neighbor to j , c_i^\dagger, c_i are the creation, annihilation operators of a spinless fermion at the site i ; $n_i = c_i^\dagger c_i$ is the occupation number at the site labelled by the vector $\mathbf{i} = (i_x, i_y)$. The vector $\mathbf{r}_{ij} = \mathbf{i} - \mathbf{j}$ is defined as the shortest vector going from the site i to the site j in a square lattice with periodic BCs. This means that $r_x \leq L/2$ and $r_y \leq L/2$ if L is even, $L \rightarrow L-1$ if L is odd. Hence, the pairwise interaction $U/|\mathbf{r}|$ exhibits a singularity on the lines $r_x = L/2$ and $r_y = L/2$ and another one at their crossing point $r_x = r_y = L/2$. $t = \hbar^2/(2ma^2)$ is the hopping term, a the lattice spacing, v_i the site potentials which are randomly distributed in the interval $[-W/2, W/2]$ and $U = e^2/(ea)$ the Coulomb interaction between two fermions separated by a in a medium of dielectric constant ϵ . When there is no disorder ($W = 0$), $\mathbf{k} = (k_x, k_y)$ being the one particle momentum, it is more convenient to write H using the Fourier transforms of the creation and annihilation operators. One has the relations

$$c_j = \frac{1}{L} \sum_{\mathbf{k}} a_{\mathbf{k}} e^{i\mathbf{k}\cdot\mathbf{j}}, \quad (2)$$

and

$$a_{\mathbf{k}} = \frac{1}{L} \sum_j c_j e^{-i\mathbf{k}\cdot\mathbf{j}}. \quad (3)$$

which yield

$$H = \sum_{\mathbf{k}} a_{\mathbf{k}}^\dagger a_{\mathbf{k}} \varepsilon(\mathbf{k}) + \sum_{\mathbf{q}, \mathbf{k}_1, \mathbf{k}_2} a_{\mathbf{k}_2 + \mathbf{q}}^\dagger a_{\mathbf{k}_2} a_{\mathbf{k}_1 - \mathbf{q}}^\dagger a_{\mathbf{k}_1} V(\mathbf{q}) \quad (4)$$

where

$$\varepsilon(\mathbf{k}) = -2t (\cos k_x + \cos k_y) \quad (5)$$

and

$$V(\mathbf{q}) = \frac{U}{2L^2} \sum_{\mathbf{r} \neq (0,0)} \frac{e^{i\mathbf{q}\cdot\mathbf{r}}}{\mathbf{r}} \quad (6)$$

Without disorder, the total momentum $\mathbf{K} = \mathbf{k}_1 + \mathbf{k}_2$ is conserved. The two particles states of different momenta are not coupled, H becoming block diagonal, each block corresponding to a given total momentum \mathbf{K} .

The dimension of the two particle Hilbert space is given by

$$N_H = \frac{M!}{N!(M-N)!} = \frac{M-1}{2} M \quad (7)$$

for $N = 2$ and $M = L^2$. When L is odd, this gives M blocks of dimension $(M-1)/2$. When L is even, we have two different dimensions of the blocks.

$$N_H = M_{b_1} M_1 + M_{b_2} M_2 \quad (8)$$

where M_1, M_2 are the number of blocks with dimensions M_{b_1}, M_{b_2} . Here,

$$M_1 = \frac{M M_{b_2} - N_H}{M_{b_2} - M_{b_1}}, \quad M_2 = \frac{N_H - M M_{b_1}}{M_{b_2} - M_{b_1}} \quad (9)$$

and

$$M_{b_1} = \frac{M}{2} - 2, \quad M_{b_2} = \frac{M}{2}. \quad (10)$$

3 The Fermi limit

When $U = W = 0$ and with periodic BCs, the states are N_H plane wave Slater determinants

$$a_{\mathbf{k}_1}^\dagger a_{\mathbf{k}_2}^\dagger |0\rangle = |\mathbf{k}_1 \mathbf{k}_2\rangle. \quad (11)$$

$k_x = (2\pi/L)n_x$ and $k_y = (2\pi/L)n_y$ with

$$n_x, n_y = \begin{cases} 0, \pm 1, \dots, \pm \frac{L-1}{2} & \text{for } L \text{ odd} \\ 0, \pm 1, \dots, \pm \left(\frac{L}{2} - 1\right), \frac{L}{2} & \text{for } L \text{ even} \end{cases} \quad (12)$$

The two particle wave functions

$$\psi(\mathbf{r}_1, \mathbf{r}_2) = \frac{1}{\sqrt{2}} \begin{vmatrix} \frac{1}{L} e^{i\mathbf{k}_1 \cdot \mathbf{r}_1} & \frac{1}{L} e^{i\mathbf{k}_1 \cdot \mathbf{r}_2} \\ \frac{1}{L} e^{i\mathbf{k}_2 \cdot \mathbf{r}_1} & \frac{1}{L} e^{i\mathbf{k}_2 \cdot \mathbf{r}_2} \end{vmatrix} \quad (13)$$

become

$$\psi(\mathbf{r}_1, \mathbf{r}_2) = \left(\frac{1}{L} e^{i\mathbf{K} \cdot \mathbf{R}} \right) \left(i \frac{\sqrt{2}}{L} \sin \mathbf{k} \cdot \mathbf{r} \right) \quad (14)$$

after the change of coordinates:

$$\mathbf{K} = \mathbf{k}_1 + \mathbf{k}_2, \quad \mathbf{k} = \frac{1}{2} (\mathbf{k}_2 - \mathbf{k}_1) \quad (15)$$

$$\mathbf{R} = \frac{1}{2} (\mathbf{r}_1 + \mathbf{r}_2), \quad \mathbf{r} = \mathbf{r}_2 - \mathbf{r}_1 \quad (16)$$

Without disorder, the motion of the center of mass and the relative motion are separable:

$$\psi(\mathbf{r}_1, \mathbf{r}_2) = \phi(\mathbf{R}) \chi(\mathbf{r}). \quad (17)$$

$\phi(\mathbf{R})$ is a plane wave of total momentum \mathbf{K} which describes the propagation of the center of mass on the 2d torus while $\chi(\mathbf{r})$ describes the relative motion. The moments $\langle |\mathbf{r}|^m \rangle$ of the inter-particle spacing \mathbf{r} are given by:

$$\langle |\mathbf{r}|^m \rangle = \int |\mathbf{r}|^m p(\mathbf{r}) d\mathbf{r} \quad (18)$$

where $p(\mathbf{r}) = |\chi(\mathbf{r})|^2$ is the inter-particle spacing distribution.

The one particle energies $\varepsilon(\mathbf{k})$ can be ordered by increasing values. The one particle GS energy ε_0 is not degenerate, while the three next excitations $\varepsilon_1, \varepsilon_2, \varepsilon_3$, are four-fold degenerate; the fourth excitation ε_4 is ten-fold degenerate; etc.

$$\begin{aligned}\varepsilon_0 &= -4t \\ \varepsilon_1 &= -2t \left(1 + \cos \frac{2\pi}{L}\right) \\ \varepsilon_2 &= -4t \cos \frac{2\pi}{L} \\ \varepsilon_3 &= -2t \left(1 + \cos \frac{4\pi}{L}\right) \\ \varepsilon_4 &= -2t \left(\cos \frac{2\pi}{L} + \cos \frac{4\pi}{L}\right) \\ &\dots\end{aligned}\quad (19)$$

The two particle GS consists of one particle of energy ε_0 and of a second particle of energy ε_1 . Because ε_1 has a four-fold degeneracy, the two particle GS energy

$$E_0 = \varepsilon_0 + \varepsilon_1 = -4t - 2t \left(1 + \cos \frac{2\pi}{L}\right) \quad (20)$$

is also four-fold degenerate.

Hereafter, we study the two particle GS of momentum $\mathbf{K} = (0, 2\pi/L)$. For $\mathbf{k}_1 = (0, 0)$ and $\mathbf{k}_2 = (0, \frac{2\pi}{L})$, the GS wave function is given by

$$\psi(\mathbf{r}_1, \mathbf{r}_2) = \left(\frac{1}{L} e^{i \frac{2\pi}{L} R_y}\right) \left(-i \frac{\sqrt{2}}{L} \sin \frac{\pi r_y}{L}\right), \quad (21)$$

which yields

$$p(r_x, r_y) = \frac{2}{L^2} \sin^2 \frac{\pi r_y}{L} \quad (22)$$

$$\langle |\mathbf{r}|^m \rangle = \frac{2}{L^2} \sum_{r_x, r_y \neq 0} (r_x^2 + r_y^2)^{m/2} \sin^2 \frac{\pi r_y}{L}. \quad (23)$$

The corresponding inter-particle spacing distribution $p(r_x, r_y)$ is shown in Fig. 1 for $L = 60$.

When one turns on the interaction U , the GS wave function of total momentum $\mathbf{K} = \mathbf{k}_i + \mathbf{k}_j$ can be written as

$$|\psi_0(U)\rangle = \sum_{i < j} a_{\mathbf{k}_i \mathbf{k}_j}(U) |\mathbf{k}_i \mathbf{k}_j\rangle \delta_{\mathbf{k}_i + \mathbf{k}_j}^{\mathbf{K}}. \quad (24)$$

The coefficients $a_{\mathbf{k}_i \mathbf{k}_j}(U) = \langle \mathbf{k}_i \mathbf{k}_j | \psi_0(U) \rangle$ can be numerically obtained if L is not too large, and the inter-particle spacing distribution $p(r_x, r_y)$ given by

$$\frac{\sum_{i < j, m < n} a_{\mathbf{k}_i \mathbf{k}_j}^* a_{\mathbf{k}_m \mathbf{k}_n} \delta_{\mathbf{k}_i + \mathbf{k}_j}^{\mathbf{K}_m + \mathbf{K}_n} [e^{i(\mathbf{k}_n - \mathbf{k}_j)r} - e^{i(\mathbf{k}_n - \mathbf{k}_i)r}]}{L^2}$$

is shown in Fig. 2 for $L = 60$, $U/t = 5$ and $\mathbf{K} = (0, 2\pi/L)$. If one particle is located at the site $(0, 0)$, one can see how the interaction localizes the second one near the site $\mathbf{r} = (L/2, L/2)$.

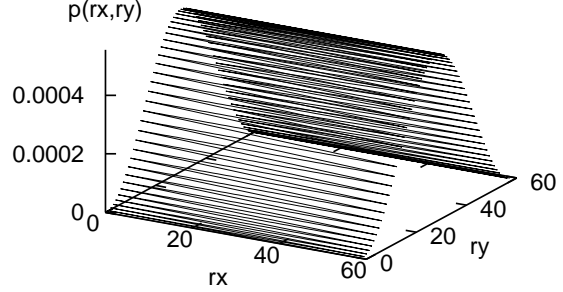


Fig. 1. Inter-particle spacing distribution $p(r_x, r_y)$ for $L = 60$, $U = 0$ and $\mathbf{K} = (0, 2\pi/L)$.

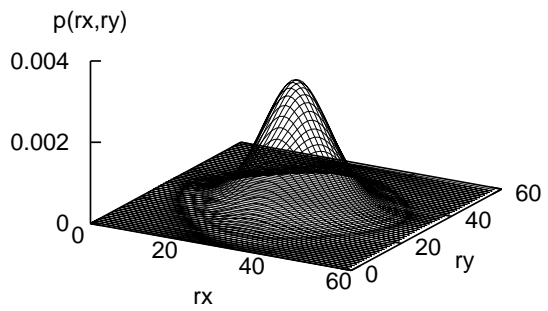


Fig. 2. Inter-particle spacing distribution $p(r_x, r_y)$ for $L = 60$, $U/t = 5$ and $\mathbf{K} = (0, 2\pi/L)$.

4 The correlated lattice limit

Before studying in more details the interaction induced localization of the inter-particle spacing \mathbf{r} , let us consider the other limit $t/U \rightarrow 0$ where the two particle wave functions $|\psi\rangle$ are more conveniently written using the operators c_i^\dagger . In this limit, the kinetic part

$$H_K = -t \sum_{\langle ij \rangle} c_i^\dagger c_j + h.c. \quad (25)$$

of H is a small perturbation compared to the Coulomb part and the levels can be expanded in powers of t/U . When $t/U \rightarrow 0$, at the order zero of a t/U expansion, the Coulomb energies E_0 and E_1 of the GS wave function $|\psi_0^{(0)}(\mathbf{K})\rangle$ and of the two degenerate first excitations $|\psi_1^{(0)}(\mathbf{K})\rangle$ and $|\psi_2^{(0)}(\mathbf{K})\rangle$ are given by

$$E_0 = \frac{U}{d_0} = \frac{\sqrt{2} U}{L} \quad (26)$$

and

$$E_1 = \frac{U}{d_1} = \frac{U}{\sqrt{\left(\frac{L}{2}\right)^2 + \left(\frac{L}{2} - 1\right)^2}} \quad (27)$$

if L is even. When L is odd, the lengths d_0 and d_1 must be differently defined:

$$d_0 = \frac{L-1}{\sqrt{2}} \quad (28)$$

and

$$d_1 = \sqrt{\left(\frac{L-1}{2}\right)^2 + \left(\frac{L-1}{2} - 1\right)^2}. \quad (29)$$

Hereafter, we assume that L is even and we consider the states of total momentum $\mathbf{K} = (0, 2\pi/L)$. $\mathbf{a} = (L/2, L/2)$, $\mathbf{b}_1 = (L/2 + 1, L/2)$ and $\mathbf{b}_2 = (L/2, L/2 + 1)$ defining the locations of three lattice sites which are as far as possible from the site $\mathbf{0} = (0, 0)$, the zero order GS wave function

$$|\psi_0^{(0)}(\mathbf{K})\rangle = \frac{1}{\sqrt{2L}} \sum_{\mathbf{j}} \exp^{i\mathbf{K}\cdot\mathbf{j}} c_{\mathbf{j}}^\dagger c_{\mathbf{j}+\mathbf{a}}^\dagger |0\rangle \quad (30)$$

is directly coupled at the order t/U to the two wave functions of energy E_1

$$|\psi_1^{(0)}(\mathbf{K})\rangle = \frac{1}{L} \sum_{\mathbf{j}} \exp^{i\mathbf{K}\cdot\mathbf{j}} c_{\mathbf{j}}^\dagger c_{\mathbf{j}+\mathbf{b}_1}^\dagger |0\rangle \quad (31)$$

and

$$|\psi_2^{(0)}(\mathbf{K})\rangle = \frac{1}{L} \sum_{\mathbf{j}} \exp^{i\mathbf{K}\cdot\mathbf{j}} c_{\mathbf{j}}^\dagger c_{\mathbf{j}+\mathbf{b}_2}^\dagger |0\rangle. \quad (32)$$

by

$$\langle \psi_1^{(0)}(\mathbf{K}) | H_K | \psi_0^{(0)}(\mathbf{K}) \rangle = -2\sqrt{2}t \quad (33)$$

and

$$\langle \psi_2^{(0)}(\mathbf{K}) | H_K | \psi_0^{(0)}(\mathbf{K}) \rangle = -\sqrt{2} \left(1 + \exp i\frac{2\pi}{L}\right) t \quad (34)$$

respectively. At the order t/U , the GS wave function is given by

$$\frac{|\psi_0^{(1)}(\mathbf{K})\rangle}{C^2} = |\psi_0^{(0)}(\mathbf{K})\rangle + |\delta\psi_0^{(1)}(\mathbf{K})\rangle \quad (35)$$

where C^{-2} is a normalization constant and

$$|\delta\psi_0^{(1)}(\mathbf{K})\rangle = \sum_{\alpha=1}^2 \frac{\langle \psi_\alpha^{(0)}(\mathbf{K}) | H_K | \psi_0^{(0)}(\mathbf{K}) \rangle}{E_0 - E_1} |\psi_\alpha^{(0)}(\mathbf{K})\rangle. \quad (36)$$

One gets

$$|\delta\psi_0^{(1)}(\mathbf{K})\rangle = A |\psi_1^{(0)}(\mathbf{K})\rangle + B |\psi_2^{(0)}(\mathbf{K})\rangle \quad (37)$$

where

$$A = 2\sqrt{2} \frac{d_0 d_1}{d_0 - d_1} \left(\frac{t}{U}\right) \quad (38)$$

$$B = \sqrt{2} \frac{d_0 d_1}{d_0 - d_1} \left(1 + \exp i\frac{2\pi}{L}\right) \left(\frac{t}{U}\right) \quad (39)$$

and

$$C^{-2} = 1 + \frac{4d_0^2 d_1^2}{(d_0 - d_1)^2} \left(3 + \cos \frac{2\pi}{L}\right) \left(\frac{t}{U}\right)^2. \quad (40)$$

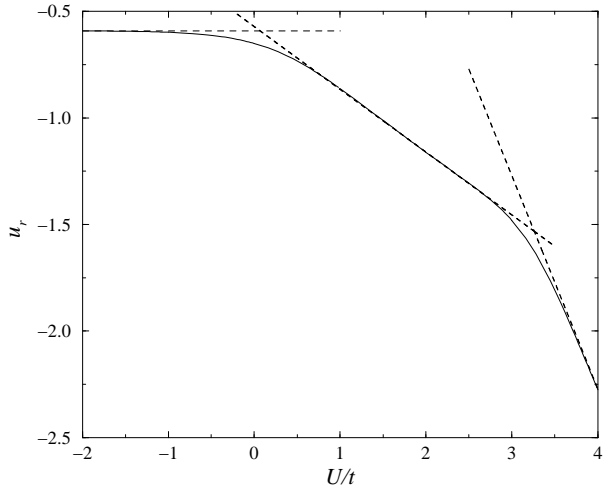


Fig. 3. Relative fluctuation u_r as a function of U for $L = 20$ and $\mathbf{K} = (0, 2\pi/L)$. The log-log plot shows the three regimes characterizing the ground state. The three dashed lines correspond to $u_r = 0.25$, $u_r \propto (U/t)^{0.31}$ and the t/U perturbative behavior given by Eq. (42).

for L even and $\mathbf{K} = (0, 2\pi/L)$. This yields for the fluctuation $\Delta r = \sqrt{\langle r^2 \rangle - \langle r \rangle^2}$ of the inter-particle spacing:

$$\Delta r = \frac{t}{U} L \sqrt{[(L-1)^2 + 1] \left(3 + \cos \frac{2\pi}{L}\right)} \quad (41)$$

and for its relative fluctuation $u_r = \Delta r / \langle r \rangle$

$$u_r = \frac{t}{U} \sqrt{2[(L-1)^2 + 1] \left(3 + \cos \frac{2\pi}{L}\right)}. \quad (42)$$

This correlated lattice behavior is shown in Fig. 3 for $L = 20$ when $U/t > 1000$.

5 The three regimes of coupling

The behavior of the relative fluctuation $u_r = \Delta r / \langle r \rangle$ is shown in Fig. 3 for $L = 20$ and $\mathbf{K} = (0, 2\pi/L)$. The crossover from independent particle towards strongly correlated motion in a finite size lattice exhibits three regimes:

- A weak U Fermi regime where u_r is large and almost independent of U . The fluctuation Δr is of the order of the expectation value $\langle r \rangle$, r being broadly distributed.
- An intermediate correlated Wigner regime where u_r exhibits a weak $(t/U)^\alpha$ decay, where $\alpha \approx 0.31$. Δr becomes small compared to $\langle r \rangle$, the distribution of r becoming narrower.
- A large U strongly correlated lattice regime where u_r exhibits the strong t/U decay predicted by the perturbative expansion (Eq. (42)), the distribution of r being extremely narrow.

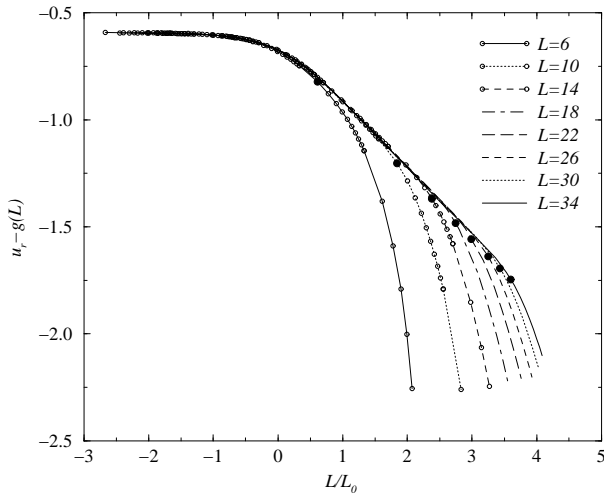


Fig. 4. Relative fluctuation $u_r - g(L)$ where $g(L) = 0.9/(L+1)^2$ as a function of $L/L_0 \approx UL/(\sqrt{8}\pi^2 t)$ for even L . The log-log plot shows the universal scaling function $F(L/L_0)$ for $U < U^*(L)$, and the non universal lattice regime for $U > U^*(L)$. The filled circles approximately give the thresholds $U^*(L)$.

The value $U^*(L)/t$ characterizing the crossover between the intermediate Wigner regime and the strongly correlated lattice regime is consistent with the condition $\Delta r < 1$. When $U \approx U^*(L)$, the lattice strongly reduces the degrees of freedom of the relative motion, and lattice expansions in powers of t/U become valid. We study in the next section the Fermi-Wigner crossover which occurs before this strongly correlated lattice regime.

6 Scaling theory of the Fermi-Wigner crossover

For $U < U^*(L)$, we define the scale L_0 associated to the interaction strength U/t such that a dimensionless observable as u_r becomes a universal function of the dimensionless ratio L/L_0 , up to certain finite size corrections which we will estimate. The argument for defining the scaling length L_0 can be presented as follows. Let us consider the system at $U = 0$ where the first particle occupies the state $\varepsilon_0 = -4t$. Due to Pauli principle, adding a second particle requires an extra kinetic energy:

$$\Delta E(U = 0) = \varepsilon_1 - \varepsilon_0 = 2t(1 - \cos(2\pi/L)) \quad (43)$$

In the other limit $t \rightarrow 0$, adding a second particle requires an extra Coulomb energy:

$$\Delta E(t = 0) = \frac{U}{d_0} \quad (44)$$

The length L_0 characterizes the scale at which $\Delta E(U = 0)$ coming from Pauli exclusion principle is equal to $\Delta E(t = 0)$ coming from Coulomb repulsion. When L is large enough, L_0 can be approximated by:

$$L_0 = \sqrt{8}\pi^2 \left(\frac{t}{U} \right), \quad (45)$$

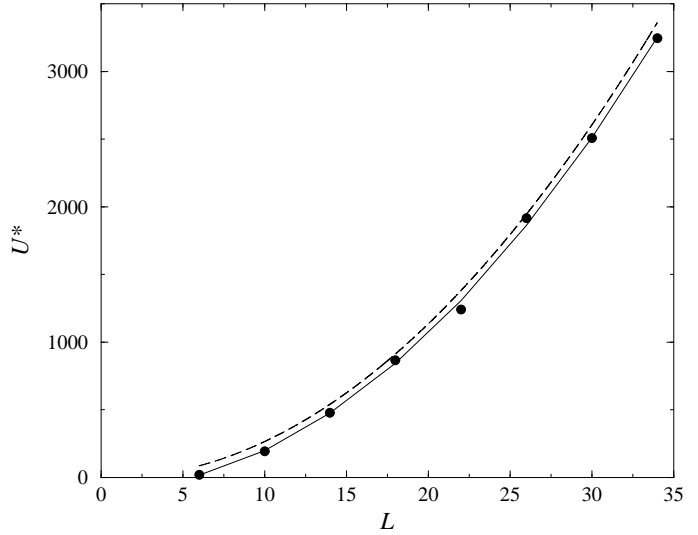


Fig. 5. Circles: Interaction thresholds $U^*(L)$ giving the end of the universal scaling regime and the beginning of the strongly correlated lattice regime, extracted from Fig. 4. The dashed line corresponds to the condition $\Delta r(U) = 2/3$ where Δr is given by Eq. (41).

but when L is small, L_0 should be more precisely determined by solving the equation $\Delta E(U = 0) = \Delta E(t = 0)$, and without neglecting the even-odd effects in the definition of d_0 . For scales $L < L_0$, the GS wave function has mainly to minimize the kinetic energy while the minimization of the Coulomb energy becomes more important for the scales $L > L_0$. The Fermi-Wigner crossover is expected at $L/L_0 = 1$.

One assumes for the dimensionless ratio u_r the usual finite size scaling ansatz [10]:

$$u_r(L, U, t) = F\left(\frac{L}{L_0}\right) + g(L), \quad (46)$$

the finite size correction $g(L) \rightarrow 0$ as $L \rightarrow \infty$. $g(L)$ can be easily evaluated when $U/t \rightarrow 0$ ($L_0 \rightarrow \infty$), the ansatz becoming

$$u_r(L, U = 0, t) = F(0) + g(L) \quad (47)$$

This is a problem without interaction where one can use Eq. (23), for eventually obtaining $F(0) = 0.2543$ and

$$g(L) \approx \begin{cases} 0.9/(L+1)^2 & \text{for } L \text{ even} \\ -0.4/(L-1)^2 & \text{for } L \text{ odd} \end{cases} \quad (48)$$

The finite size correction $g(L)$ has a sign which depends on the parity of L and disappears as the inverse of the total number of lattice sites.

Fig. 4 gives $F(L/L_0) = u_r - g(L)$ for even values of L . One can see the universal scaling behavior with a Fermi Wigner crossover at $L = L_0$ up to a value $U^*(L)$ denoted by the filled circles where scaling breaks down and the correlated lattice regime begins. The behavior of $U^*(L)$ is shown in Fig. 5, where one can see that the values $U^*(L)$

extracted from Fig. 4 are precisely given by the condition $\Delta r \approx 2/3$, Δr being given by Eq. (41). Below $U^*(L)$, $u_r - g(L)$ is a one parameter function of $L/L_0 \propto LU/t$, and the lattice effects are irrelevant. The lattice regime occurs only above a large interaction $U^*/t \propto L^2$ when L is large.

For N spinless fermions in a $L \times L$ square lattice, the Coulomb energy to Fermi energy ratio becomes [11]:

$$r_s = \frac{U}{2t} \frac{1}{\sqrt{\pi\nu}} \quad (49)$$

for a density $\nu = N/L^2$. As it must be, the dimensionless ratios L/L_0 and r_s are proportional, the advantage of using L/L_0 instead of r_s being that the crossover occurs when $L/L_0 = 1$, and not at $r_s = 1$. In the strongly correlated lattice regime, u_r becomes a function of Lt/U , and not of $r_s \propto LU/t$.

The Fermi-Wigner universal crossover is illustrated with more details in Fig. 6 where we have only taken even values of L . One can see that the finite size correction $g(L) = 0.9/(L+1)^2$ allows us to plot all the values $u_r - g(L)$ calculated for $U < U^*(L)$ onto the universal scaling curve $F(L/L_0)$ when $L = 6, 10, \dots, 60$. Fig. 7 gives the same universal curve $F(L/L_0)$ for the odd values of L , once the finite size correction $g(L) = -0.4/(L+1)^2$ have been subtracted to u_r . The universal function $F(x)$ is close to its value $F(0) = 0.2543$ when $x \leq 1$ and behaves as $x^{-\alpha}$ with $\alpha \approx 0.31$ when $x \geq 1$.

The value $\alpha \approx 0.31$ depends on the exact form of the pairwise repulsion $U/|\mathbf{r}|$ around $\mathbf{r} = (L/2, L/2)$. Due to our definition of the inter-particle spacing r , $U(r)$ is non analytic around $\mathbf{r} = (L/2, L/2)$, making the study a little bit involved. If one modifies the pairwise repulsion such that $U(r)$ becomes analytic around $(L/2, L/2)$, taking for instance

$$U(\mathbf{r}) = \frac{U}{\frac{L}{\pi} \sqrt{\sin^2\left(\frac{r_x\pi}{L}\right) + \sin^2\left(\frac{r_y\pi}{L}\right)}} \quad (50)$$

instead of $U/|\mathbf{r}|$, one can show [12] that the equation for the relative motion becomes identical to the single particle motion in a 2d harmonic potential when U is large enough, to eventually obtain a slightly different exponent $\alpha = 1/4$ in the continuous limit ($L \rightarrow \infty$).

7 Effects of a weak random substrate

We now study the effect of random site potentials v_i upon the Fermi-Wigner crossover. We restrict our study to the limit of weak disorder, the values of W being large enough to yield one particle diffusive dynamics in the non interacting system, but too small to yield one particle Anderson localization. In the presence of disorder, the momenta \mathbf{K} are not conserved, and we need to diagonalize the total Hamiltonian H given by Eq. (1) in the site basis $c_i^\dagger c_j^\dagger |0\rangle$. Moreover, the relative fluctuations u_r are now random variables, and the ensemble average values $\langle u_r \rangle$ will be considered.

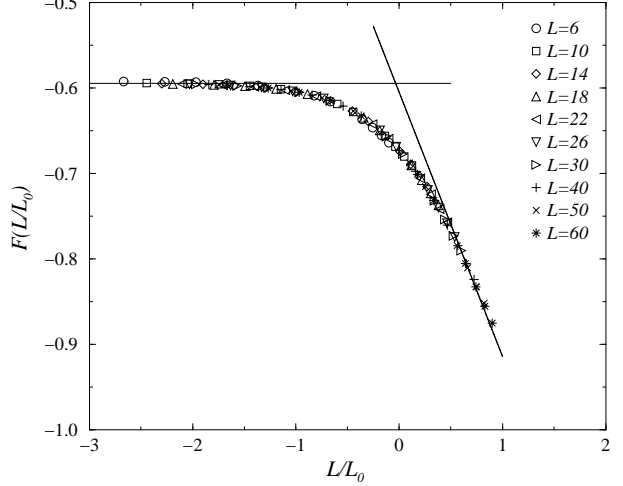


Fig. 6. Fermi-Wigner crossover for the relative fluctuation u_r , described by the universal scaling function $F(L/L_0) = u_r - g(L)$ in a log-log plot. Values calculated from even values of L with the finite size correction $g(L) = 0.9/(L+1)^2$. The solid lines correspond to $F(x) = 0.2543$ and $F(x) \propto x^{-0.31}$ respectively.

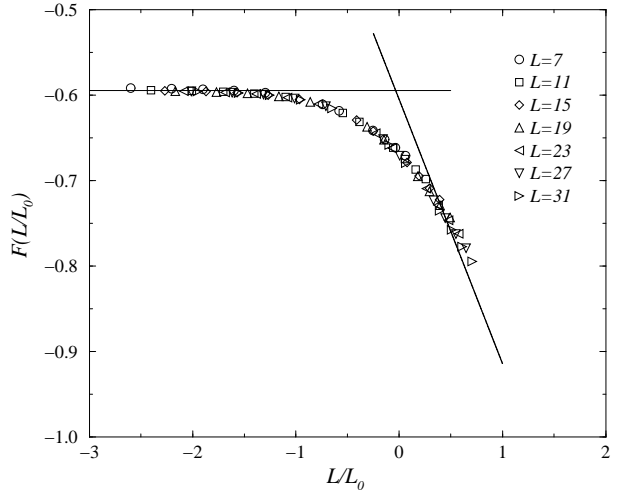


Fig. 7. Fermi-Wigner crossover for the relative fluctuation u_r , described by the universal scaling function $F(L/L_0) = u_r - g(L)$ in a log-log plot. Values calculated for odd values of L with the finite size correction $g(L) = -0.4/(L-1)^2$.

Figure 8 shows for $L = 14$ the difference between the u_r obtained for $W = 0$ and the $\langle u_r \rangle$ calculated for $1 \leq W \leq 4$. One can see that the disorder reduces the relative fluctuations $\langle u_r \rangle$, shifts the Fermi-Wigner crossover to weaker interactions, and reduces the exponent α characteristic of the $U^{-\alpha}$ decay for intermediate interactions.

For a weak value of W and small enough values of U/t to avoid the correlated lattice regime, we assume the generalized scaling ansatz :

$$\langle u_r(L, U, t, W) \rangle = F_W \left(\frac{L}{L_W(U, t, W)} \right) + g_W(L). \quad (51)$$

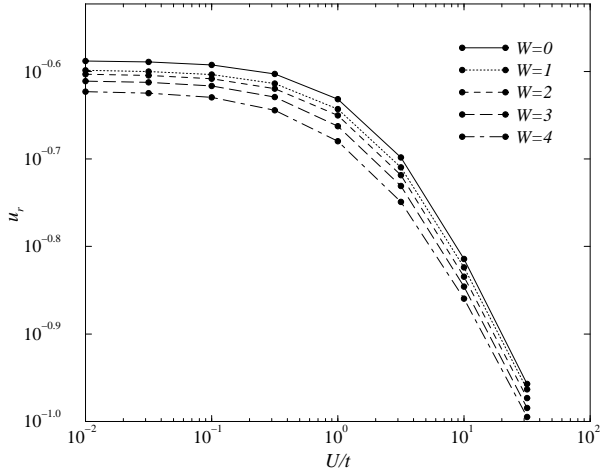


Fig. 8. Ensemble average relative fluctuation $\langle u_r \rangle$ as a function of U/t for $L = 14$ and $W = 0, 1, 2, 3, 4$ in a log-log plot.

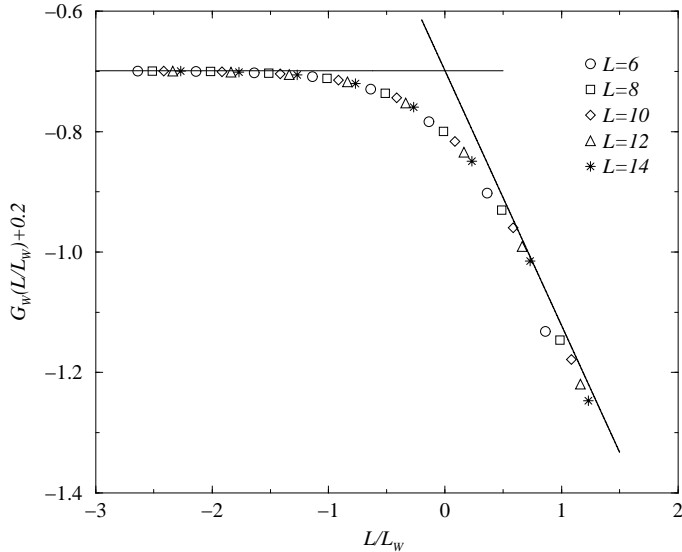


Fig. 9. Scaling function $G_W(L/L_W) + C$ for $W = 2$ and $6 \leq L \leq 14$. An arbitrary constant $C = 0.2$ has been taken for the log-log plot.

Since

$$\langle u_r(L, U = 0, t, W) \rangle = F_W(0) + g_W(L), \quad (52)$$

which implies that

$$G_W = \langle u_r(L, U, t, W) \rangle - \langle u_r(L, U = 0, t, W) \rangle \quad (53)$$

must only depend on the ratio L/L_W . The scaling length L_W is defined in such a way that the Fermi-Wigner crossover remains at $L/L_W = 1$. As shown in Fig. 9, all the data calculated for $L = 8, 10, 12, 14$ can be mapped onto the same scaling curve $G_W(L/L_W) = F_W(L/L_W) - F_W(0)$. We just show the curve $G_W=2(L/L_W)$, the curves obtained for $W = 1, 2, 3, 4$ being also consistent with the ansatz (51) when U and L are varied in the same range. $G_W(x) \approx 0$ for $x < 1$ while $G_W(x) \approx x^{-\alpha(W)}$ for $x > 1$,

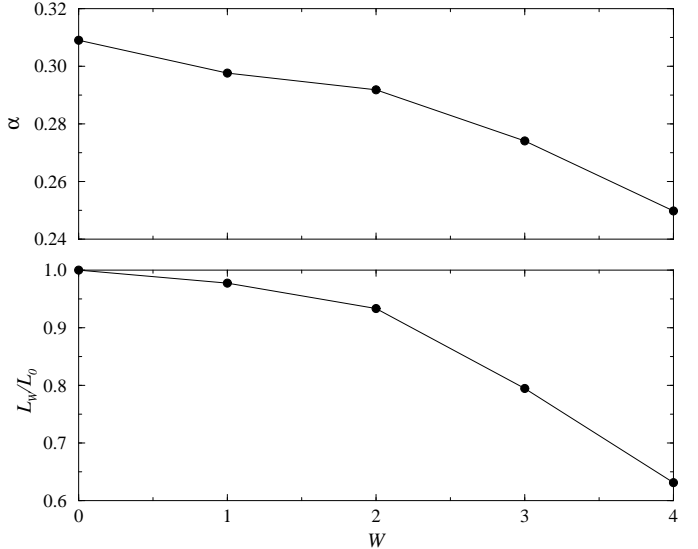


Fig. 10. As a function of W , exponent $\alpha(W)$ characterizing the scaling function $G_W(x) \propto x^{-\alpha(W)}$ when $x > 1$ (upper figure) and reduction factor L_W/L_0 for the scaling length L_W (lower figure).

the exponent $\alpha(W)$ being given in upper Fig. 10. To obtain that the Fermi-Wigner crossover remains at $L/L_W = 1$, one needs to take the scaling lengths L_W , the reduction factors L_W/L_0 being given in the lower Fig. 10.

The reduction of the crossover scale L_W by the random potentials can be qualitatively explained if we revisit the argument which has allowed us to define L_0 without disorder: $L = L_W$ when the energies ΔE_W which are necessary for adding a second particle in the one particle system are the same in the two limits $U = 0$ and $t = 0$. On one hand, when $U = 0$, the first one particle excitation has a fourfold degeneracy which is removed by disorder. This gives a reduction of the energy cost $\langle \Delta E_W(U = 0) \rangle$ necessary in the Fermi limit. On the other hand, the energy cost $\langle \Delta E_W(t = 0) \rangle$ necessary in the Coulomb limit remains almost unchanged if W is weak. This gives a shift of the Fermi-Wigner crossover to a lower scale $L_W < L_0$ in the limit of a weak disorder. In Fig. 11, we have plotted as a function of L for $W = 0$ and $W = 2$ the disorder averaged energies $\langle \Delta E_W(U = 0) \rangle$ and $\langle \Delta E_W(t = 0) \rangle$. One can see indeed that $\langle \Delta E_W(U = 0) \rangle$ is decreased by the disorder, while $\langle \Delta E_W(t = 0) \rangle$ remains essentially unchanged. The curves cross at $L = L_0 \approx 8.9$ when $W = 0$ and $L = L_W \approx 7.1$ when $W = 2$. The obtained ratio $L_W=2/L_0 \approx 0.8$ is indeed smaller than 1, though somewhat below the value $L_W=2/L_0 \approx 0.9$ given in Fig. 10.

This quantitative disagreement may be due the distributions of the considered random variables. We have considered only the ensemble average behaviors, which may not give the typical scaling behaviors, both for the relative fluctuations and for the energies. When $U = 0$, it is indeed well known that the level spacing distributions are not normally distributed, but depend on the nature of the one particle dynamics. In the bulk of the spectrum,

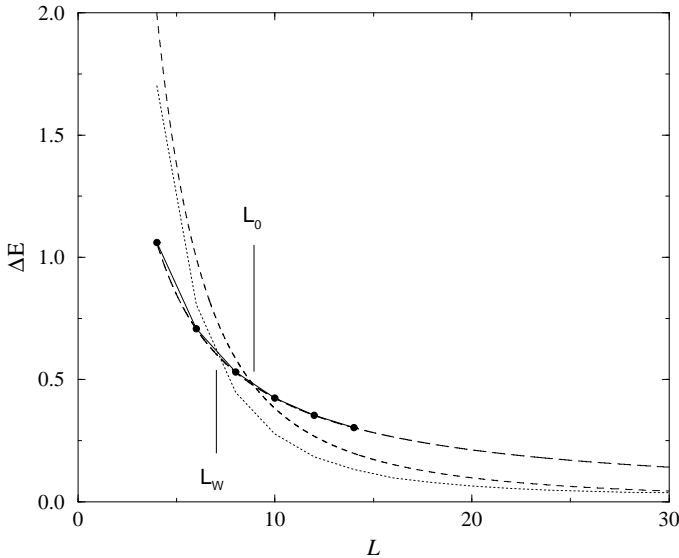


Fig. 11. As a function of L , curves $\Delta E(U = 0, t = 1, W = 0)$ (dashed line) and $\Delta E(U = 3, t = 0, W = 0)$ (long dashed line) crossing at $L = L_0$, and ensemble average curves $\langle \Delta E(U = 0, t = 1, W = 2) \rangle$ (dotted line) $\langle \Delta E(U = 3, t = 0, W = 2) \rangle$ (filled circle) crossing at $L = L_w$. $L_0(t/U) \approx 8.9$ and $L_w(t/U) \approx 7.1$.

one has typically a Poisson distribution if the dynamics is ballistic and non chaotic, a Wigner-Dyson distribution if the dynamics is diffusive, a Poisson distribution again when one has Anderson localization. Near the one particle spectrum edges, the distribution can differ from the bulk distribution. This is why an argument based on disorder average quantities can only qualitatively give the disorder induced reduction of the scaling length.

In conclusion, let us underline that an Hamiltonian with three parameters, U , t and W , has many different limits. This section is restricted to the study of the competition between the interaction U and the kinetic energy t when the disorder W remains a weak perturbation, in the limit $L < L_1$, L_1 denoting the one particle localization length. In this limit, we have shown that $\langle u_r \rangle$ is still given by a function F_W of the dimensionless ratio L/L_W and that the scaling length L_W decreases as a function of W . This is in agreement with the general idea that a random substrate favors charge crystallization [11,13], the correlated motion persisting to larger densities (weaker values of r_s). But for larger W , the issue is to describe the crossover from a Fermi glass of Anderson localized states towards a Wigner glass. In this strongly disordered limit, the u_r will have large sample to sample fluctuations, and one cannot rule out that the average $\langle u_r \rangle$ will finish to be meaningless or that the one parameter scaling function $F_W(L/L_W)$ could become a more complicated two parameter scaling function of L/L_0 and L/L_1 . The study of those glassy behaviors is left for another study.

CONACyT-Mexico and CEA have supported M. Martínez during the time this research was performed in Saclay. We thank Z. Á. Németh for useful discussions.

References

1. R. Egger, W. Häusler, C.H. Mak and H. Grabert, Phys. Rev. Lett. **82**, 3320 (1999).
2. C. Yannouleas and U. Landman, Phys. Rev. Lett. **82**, 5325 (1999).
3. C. Yannouleas and U. Landman, Phys. Rev. Lett. **86**, 1726 (2000).
4. C. Yannouleas and U. Landman, Phys. Rev. **B 61**, 15895 (2000).
5. A. Matulis and F. M. Peeters, cond-mat/0005299.
6. J. Kyriadidis, M. Pioro-Ladrière, M. Cioga, A.S. Sachrajda and P. Hawrylak, cond-mat/0111543.
7. A.V. Filinov, M. Bonitz and Yu.E. Lozovik, Phys. Rev. Lett. **B 86**, 3851 (2001).
8. L. Jacak, P. Hawrylak and A. Wojs, Quantum dots, (Springer-Verlag, Berlin Heidelberg, 1998).
9. I.V. Schweigert, V.A. Schweigert and F.M. Peeters, Phys. Rev. Lett. **84**, 4381 (2000).
10. M.E. Fisher and M.N. Barber, Phys. Rev. Lett. **28**, 1516 (1972); J.-L. Pichard and G. Sarma, J. Phys. C: Solid State Physics **14**, L127 and L617 (1981) and refs. therein.
11. G. Benenti, X. Waintal, and J.-L. Pichard, Phys. Rev. Lett. **83**, 1826 (1999).
12. Z. Á. Németh, unpublished.
13. S.T. Chui and B. Tanatar, Phys. Rev. Lett. **74**, 458 (1995).